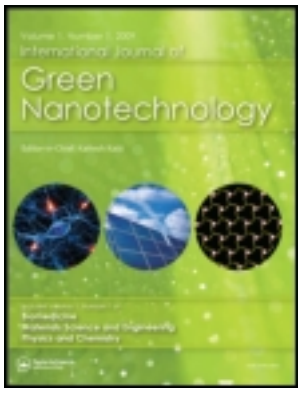

International Journal of Green Nanotechnology
Publication details, including instructions for authors and subscription information:
http://www.tandfonline.com/loi/ugnj20

Areca catechu Linn.-Derived Silver Nanoparticles: A Novel Antitumor Agent against Dalton's Ascites Lymphoma

Raman Sukirtha [a], Muthukalingan Krishnan [a], Rajamanickam Ramachandran [a], Soundararajan Kamalakkannan [b], Palanivel Kokilavani [a], Devaraj SankarGanesh [a], Soundarapandian Kannan [c] & Shanmugam Achiraman [a]

[a] Department of Environmental Biotechnology, School of Environmental Sciences, Bharathidasan University, Tiruchirappalli, Tamilnadu, India

[b] Department of Animal Science, Bharathidasan University, Tiruchirappalli, Tamilnadu, India

[c] Department of Zoology, Bharathiar University, Coimbatore, Tamilnadu, India

Available online: 27 Jul 2011

To cite this article: Raman Sukirtha, Muthukalingan Krishnan, Rajamanickam Ramachandran, Soundararajan Kamalakkannan, Palanivel Kokilavani, Devaraj SankarGanesh, Soundarapandian Kannan & Shanmugam Achiraman (2011): *Areca catechu* Linn.-Derived Silver Nanoparticles: A Novel Antitumor Agent against Dalton's Ascites Lymphoma, International Journal of Green Nanotechnology, 3:1, 1-12

To link to this article: http://dx.doi.org/10.1080/19430892.2011.571626

International Journal of Green Nanotechnology, 3:1–12, 2011

ISSN: 1943-0892 print / 1943-0906 online
DOI: 10.1080/19430892.2011.571626

BIOMEDICINE

Areca catechu Linn.–Derived Silver Nanoparticles: A Novel Antitumor Agent against Dalton's Ascites Lymphoma

Raman Sukirtha
Muthukalingan Krishnan
Rajamanickam Ramachandran
Soundararajan Kamalakkannan
Palanivel Kokilavani
Devaraj SankarGanesh
Soundarapandian Kannan
Shanmugam Achiraman

Received 30 January 2011 and accepted 4 February 2011.
We gratefully acknowledge University Grant Commission, University Grant Commission-Special Assistance Programs, Department of Science and Technology Fast Track Scheme, Department of Science and Technology-Nano Mission, Council for Scientific and Industrial Research, government of India for their financial support. The authors thank Bharathidasan University, Tiruchirappalli, Tamilnadu, for the University Research Fellowship. The authors report no conflict of interest. The authors alone are responsible for the content and writing of the article.

Raman Sukirtha, Muthukalingan Krishnan, Rajamanickam Ramachandran, Palanivel Kokilavani, Devaraj SankarGanesh, and Shanmugam Achiraman are affiliated with the Department of Environmental Biotechnology, School of Environmental Sciences, Bharathidasan University, Tiruchirappalli, Tamilnadu, India.
Soundararajan Kamalakkannan is affiliated with the Department of Animal Science, Bharathidasan University, Tiruchirappalli, Tamilnadu, India.
Soudarapandian Kannan is affiliated with the Department of Zoology, Bharathiar University, Coimbatore, Tamilnadu, India.
Address correspondence to Dr. S. Achiraman, Info Chemicals and Nano Oncology Lab, Department of Environmental Biotechnology, School of Environmental Sciences, Bharathidasan University, Tiruchirappalli 620 024, Tamilnadu, India. E-mail: achiramans@gmail.com

ABSTRACT. The present investigation emphasizes biomimetic synthesis of silver nanoparticles (AgNPs) using an aqueous extract of *Areca catechu* and its impact on a Dalton's ascites lymphoma (DAL) mice model. The ultraviolet (UV) spectrum of AgNPs at 428 nm confirmed the spherical shape of the particles and average size of 80 nm was determined using electron microscopic analysis. Elemental silver and adhered biomolecules conferred a synergetic antitumor activity with a significant increase in life span of tumor-induced mice with decreased body weight and tumor volume. Acridine Orange staining and DNA fragmentation studies of harvested tumor cells showed higher level of cytotoxicity by AgNPs when compared to aqueous extract of *Areca catechu*.

KEYWORDS. silver nanoparticles, *Areca catechu*, Dalton's ascites lymphoma

INTRODUCTION

In outward appearance, colloidal nanoparticles (NPs) prevail over the conventional antitumor drugs that conferred resistance in tumor cells. Colloidal NPs also reduces its toxicity toward normal cells by increasing their selectivity toward cancer cells. In this regard, a potential entrant is silver nanoparticles (AgNPs) with the possibility for use as a therapeutic agent in cancer therapy.[1] In biomimetics research, biological sources are used for eco-friendly, reliable metal nanoparticles synthesis.[2] Over the past decade, the use of biological systems such as yeast, fungi, bacteria, and plants has been reported for their nanoparticles synthesis. Some of the well-known examples are extracellular synthesis of AgNPs by a silver-tolerant yeast strain MKY3[3] and biosynthesis of silver-based crystalline nanoparticles from *Pseudomonas stutzery* AG259 isolated from silver mines.[4] Eukaryotic organisms such as fungi have also been used to grow nanoparticles.[5] Though the synthesis of metal nanoparticles from microorganisms continues to be investigated, the use of plants is an exciting possibility that is unexplored and underexploited. Biocompatible synthesis of NPs by plants would be advantageous over other processes by eliminating the elaborate cell cultures.[6] The era of green-synthesized NPs such as gold and silver from plants was first reported by Gardea-Torresdey et al.[7] Consequently, the synthesis of AgNPs from natural products such as black tea,[8] *Aloe vera* plant extract,[9] lemon grass,[10] neem leaf extract,[11] green tea,[12] etc., is well established.

Since the fourth century, *Areca catechu* (*Areca* nut), commonly known as *betel nut*, has been a popular masticatory throughout the world.[13] The nuts, husks, young shoots, buds, and leaves have been used in various medicinal preparations and the nut possesses curative abilities against many diseases such as obesity, leprosy, anemia, and leukoderma.[14] The presence of total phenolics and tannins in the *Areca* nut is well documented and reflects their potential antioxidant properties.[15] To date no reports have been documented for *A. catechu*–derived AgNPs synthesis and the study of antitumor activity of biosynthesized AgNPs is in evolutionary phase. Hence, the present study highlights the synthesis of AgNPs from *A. catechu* nut and antitumor activity against Dalton's ascites lymphoma (DAL)-induced mice model.

RESULTS AND DISCUSSION

Environmentally friendly methodologies have been gradually implemented due to their feasibility in the synthesis of nanostructures.[16] We focused on the biosynthesis of AgNPs using *A. catechu* aqueous extract and its antitumor activity was studied against a DAL-induced mice model. Applying the principle of green chemistry, the bioreduction of silver nitrate with aqueous extract of *A. catechu* at various temperatures (30, 60, 90, 95°C) for an incubation time of 10 min resulted in the formation of AgNPs at an ambient temperature of 95°C.

Confirmation of AgNPs Synthesis

Formation of yellowish brown color at an ambient temperature of 95°C confirmed the synthesis of AgNPs (Figure 1A). A color change

FIGURE 1. (a) Color intensity of *A. catechu*–derived colloidal AgNPs. (b) UV-Vis spectrum of biosynthesized AgNPs with a specific plasmonic resonance at 428 nm 95°C. (Color figure available online.)

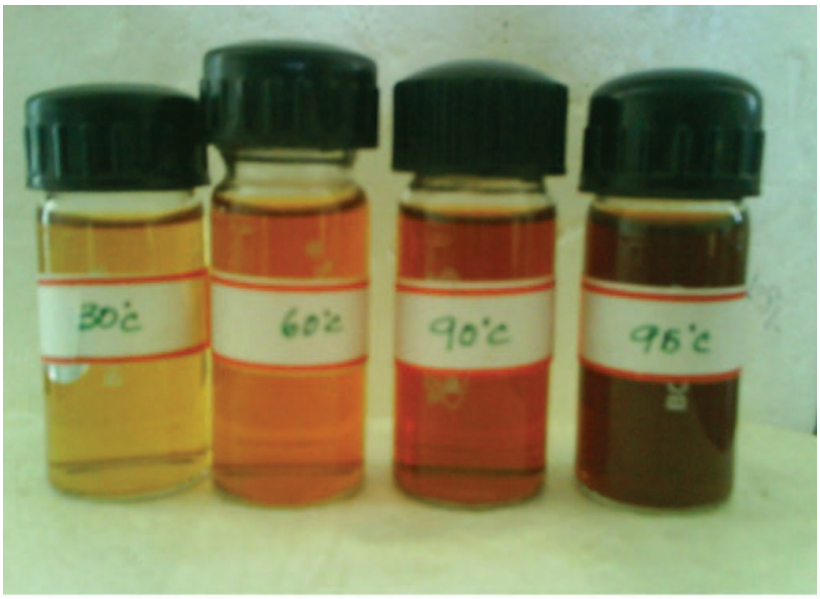

(a)

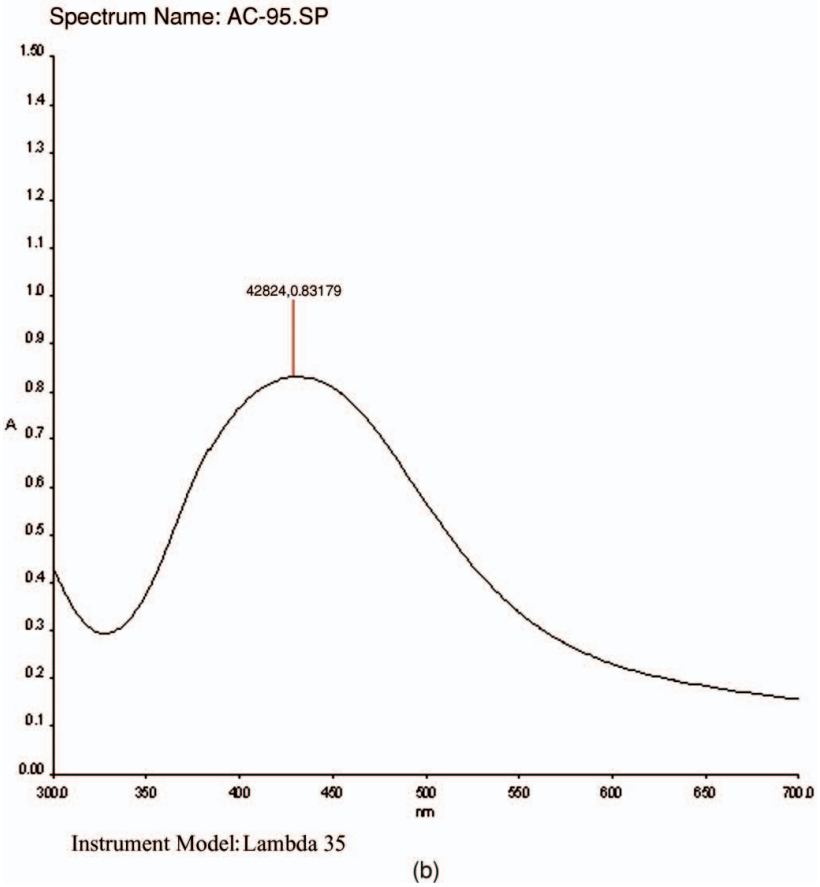

(b)

arose due to the excitation of surface plasmon vibration in the synthesized nanoparticles. With this color intensity evident, it was confirmed that more than 90% formation of AgNPs was achieved at 95°C compared to the other temperatures. A notorious color change indicated the synthesis of AgNPs at 95°C and similar results were observed by Shankar et al.[17] in aqueous neem leaf broth. The biosynthesized AgNPs were confirmed by their plasmonic resonance peak at 428 nm in ultraviolet-visible (UV-Vis) spectroscopic analysis (Figure 1B). In UV-Vis analysis, a maximum peak at 428 nm revealed a positive correlation between temperature and AgNPs synthesis. In addition, AgNPs synthesis is directly proportionate to reaction temperature.[18,19] Further, the size and shape of nanoparticles was studied by UV-Vis spectroscopic analysis. In the present study, spherical-shaped AgNPs were obtained at ambient temperature. Wiley et al.[20] reported that the peak at ∼430 nm could be assigned to the plane dipole resonance of AgNPs, indicating the presence of spherical particles with small diameters. The optical absorption spectrum of AgNPs was dominated by the surface plasmon resonance (SPR) band, which exhibits a shift toward the red or blue end depending upon the particle size, shape, state of aggregation, and surrounding dielectric medium.[21] Thus, in our study the synthesis of spherical-shaped AgNPs with a blue shift was initially confirmed with the UV-Vis spectral results.

Characterization of Biosynthesized AgNPs

According to the results observed in UV-Vis spectroscopy, the temperature at which maximum synthesis was obtained was passable for further structural characterization and particle size determination using scanning electron microscopy (SEM) and transmission electron microscopy (TEM) analysis, respectively. The nanoparticles were uniformly distributed and most of the particles were spherical in shape (Figure 2A). In the present study, SEM observation showed polydispersed AgNPs with a spherical shape, which was highly similar to the topological reports of Song et al.[19] The images showed a broad size distribution of particles ranging from 20 to 150 nm, with an average around 80 nm (Figure 2B). TEM results confirmed the average particle size and these obtained results showed a similar outcome as that in Mukherjee et al.[22] A similar trend was also noticed in the TEM images of gold nanoparticles obtained from 5% persimmon leaf broth and 1 mM $HAuCl_4$ solution at various temperatures.[19] Therefore, the temperature was found to be the baseline to determine the synthesis rate and size of the AgNPs.

Characterization of Associated Molecules

Energy-dispersive X-ray (EDX) analysis revealed strong signal in the silver region 3 keV confirming the presence of elemental silver (Figure 3A). This compositional analysis of biosynthesized AgNPs showed the presence of carbon, oxygen, and hydrogen counts along with AgNPs. An optical absorption band peak was observed in the range of 3–4 keV, which is typical for the absorption of silver nanocrystallites. Similarly, a sharp band at 3 KeV observed in this study confirmed the presence of elemental silver. In contrast, the weak signals present along with the silver revealed the presence of carbon, oxygen, and hydrogen elements, which reflect the intensity of active biomolecules along with the biosynthesized AgNPs. It has also been reported that biosynthesized nanoparticles using plant extracts are bounded by a thin layer of some capping organic material obtained from the plant leaf broth.[23,24]

Further, the bioactive compounds in aqueous extract of *A. catechu* responsible for bioreduction of silver nitrate into AgNPs were confirmed with their by their Fourier transform infrared (FTIR) band peaks. The presence of polyphenolics such as terpenoids, flavonoids, and tannic acid was confirmed with their corresponding band peaks at 3580 and 3314 cm^{-1}.The presence of proteins was confirmed with the amide bond stretch of C-O and C-N groups with peaks at 1634 and 1352 cm^{-1} (Figure 3B). It was evidenced that biomolecules such as flavans and tannins were present in a remarkable content in aqueous extract of *A. catechu*.[25] In addition, the presence of polyphenolics was confirmed by band peaks at 3580 and 3314 cm^{-1}, which

FIGURE 2. (a) Topographical appearance of biosynthesized AgNPs in SEM analysis. (b) TEM image of biosynthesized AgNPs showing average particle size of 80 nm.

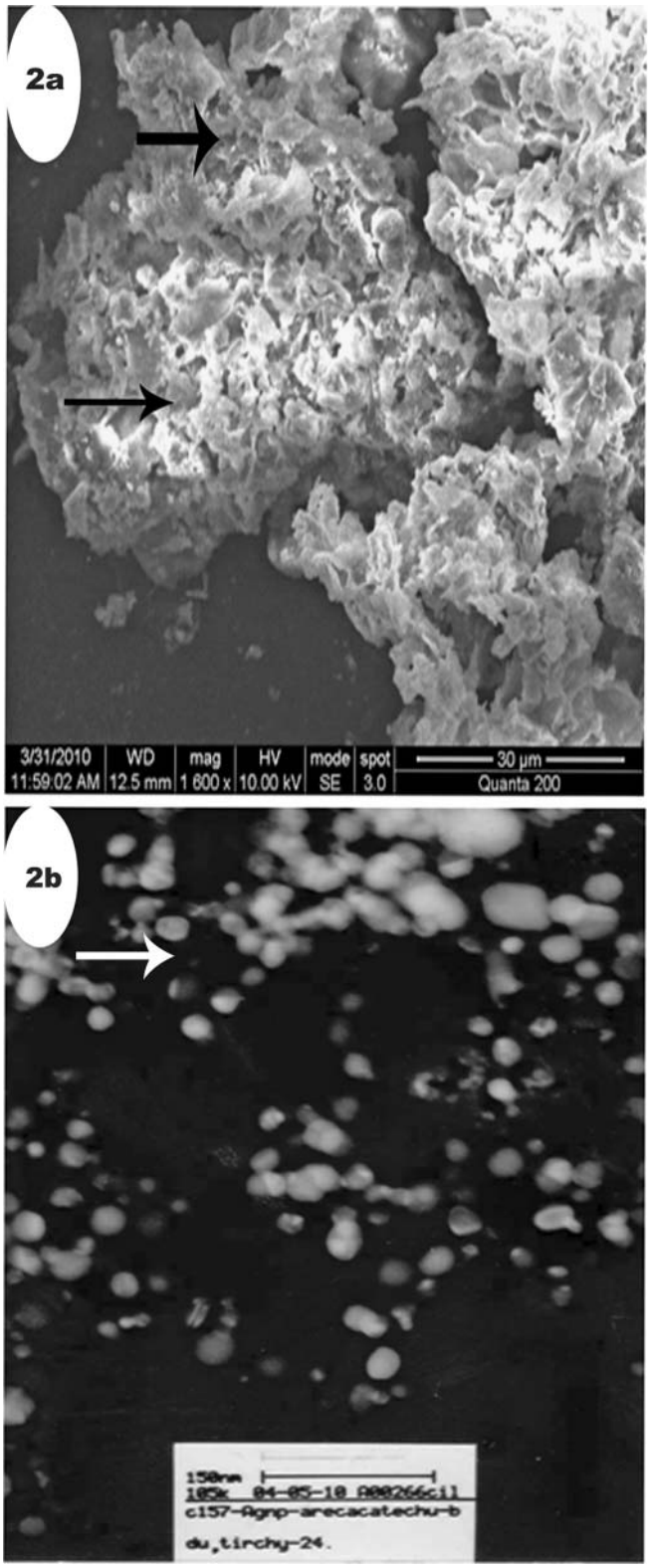

FIGURE 3. (a) Strong signal of elemental silver at 3 KeV in EDX analysis. (b) FTIR spectra of phytochemicals-coated colloidal AgNPs. (Color figure available online.)

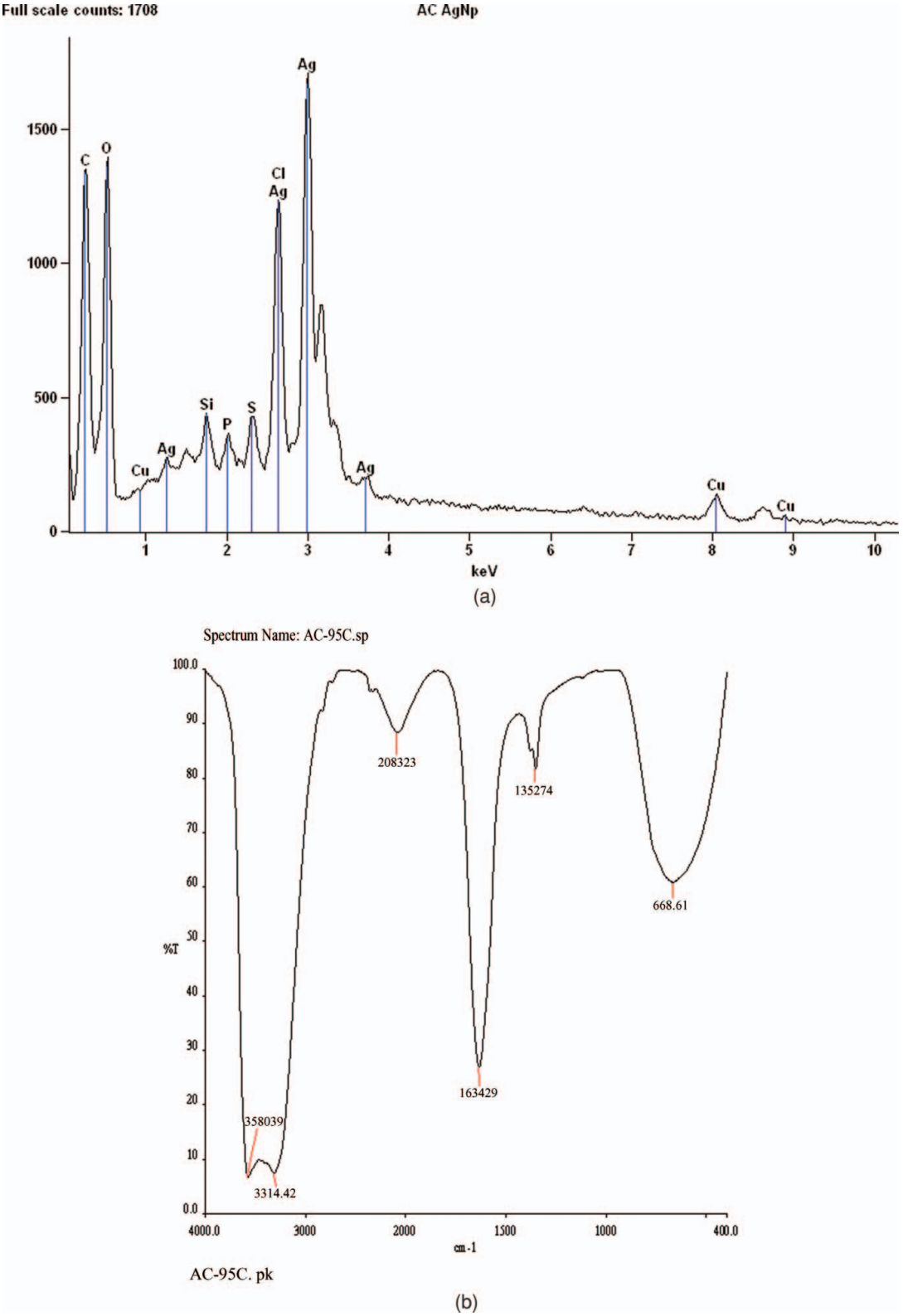

arose due to the sharp and free O-H bond. The biomolecules responsible for the reduction of silver ions may be the presence of flavanoids and terpenoids.[17] The band peaks at 1634 and 1352 cm^{-1} developed for C-C and C-N stretching, respectively, reflect the presence of proteins. In the current study the presence of C=O stretching mode indicated the presence of a –COOH group in the material bound to AgNPs. Similar findings the presence of proteins as ligands for AgNPs and a factor for increasing the stability of AgNPs.[26] Thus, the FTIR bands at 1634 and 1352 cm^{-1} indicated the possibility of AgNPs bound to proteins through free amine groups. The obtained results showed the potential of these biomolecules as dependable for efficient stabilization of AgNPs synthesized using *A. catechu*. The cytotoxic and antitumor properties of the biosynthesized AgNPs might have a synergetic effect along with the bound compounds such as flavans and proteins, which possess antitumor activity.[27]

In Vivo Anti Tumor Activity of Biosynthesized AgNPs

In vivo study of AgNPs against DAL tumor cells resulted in a significant decrease in

FIGURE 4. (a) Histogram of significantly decreased tumor volume in AgNPs treated groups compared to tumor group. Results are represented as a mean with bars showing the standard deviation. (b) Histogram representation of significant increase in life span of experimental groups compared to tumor group. Results are represented as a mean with bars showing the standard deviation. (c) Histogram representation of revival of normal body weight in the experimental groups compared to the tumor group. Results are represented as a mean with bars showing the standard deviation. (Color figure available online.)

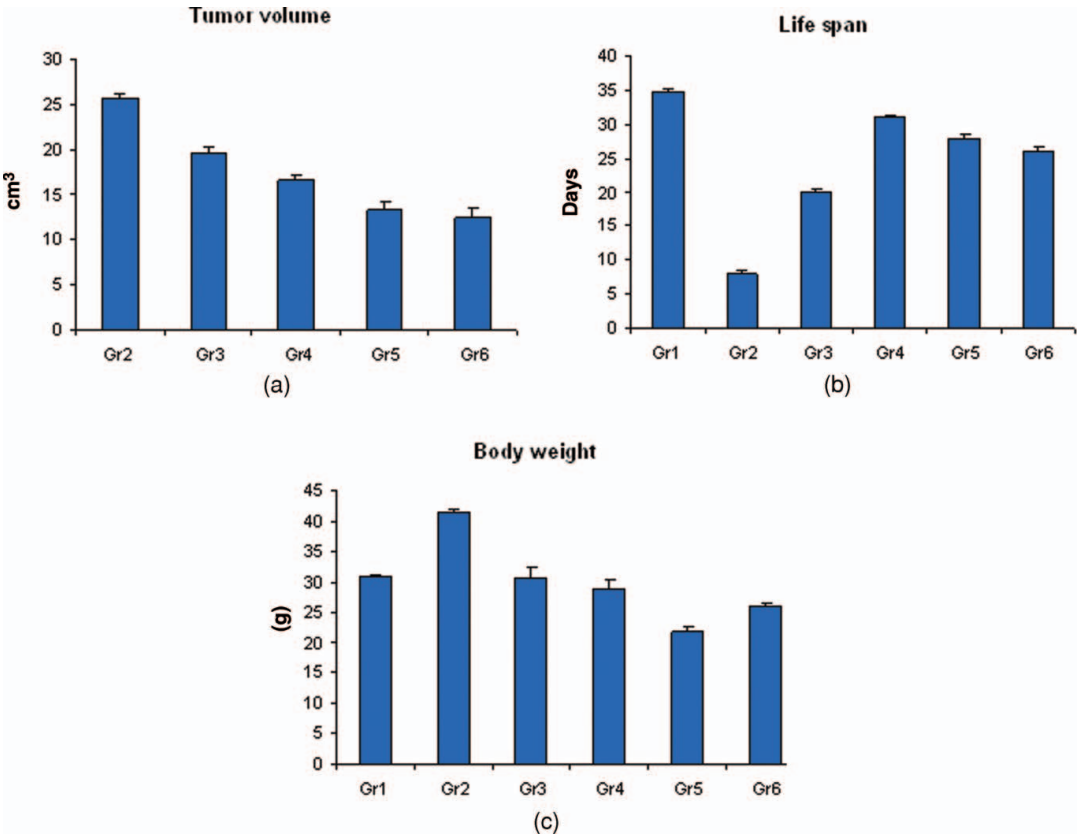

tumor volume; however, the impact was greater in the AgNPs-treated group compared to the aqueous extract–treated and untreated tumor groups (Figure 4A). Supporting the above results, Badami et al.[28] stated that DAL tumor mice had increased ascites tumor volume. Reduction in tumor volume reflects the direct efficacy of chemotherapy and immunotherapy with the indications of natural immune response.[29] A significant increase in the life span of DAL model mice confirmed the antitumor activity of biosynthesized AgNPs (Figure 4B). To conclude the overall therapeutic response we also monitored body weight as a preliminary indicator for all experimental groups throughout the entire period of treatment. In our results, AgNPs treated DAL bearing mice exhibited a significant reduction in body weight than the control and aqueous-treated groups (Figure 4C). These results were consistent with previous reports of Chanda et al.[29] The nanoparticles are potential indicators for antitumor activity and could act specifically on the biomarkers present in the cancer cells.[30] Biosynthesized AgNPs using aqueous extract of *A. catechu* resulted in an average particle size of ∼80 nm. There are reports suggesting that

FIGURE 5. (a) Viable DAL cells exhibiting uniform green fluorescence. (b) Early apoptosis in DAL cells treated with *A. catechu* extract exhibiting orange fluorescence. (c)–(e) Prominent membrane blebbing and nuclear condensation with apoptotic bodies exhibiting orange to red fluorescence in AgNPs-treated DAL cells. (Color figure available online.)

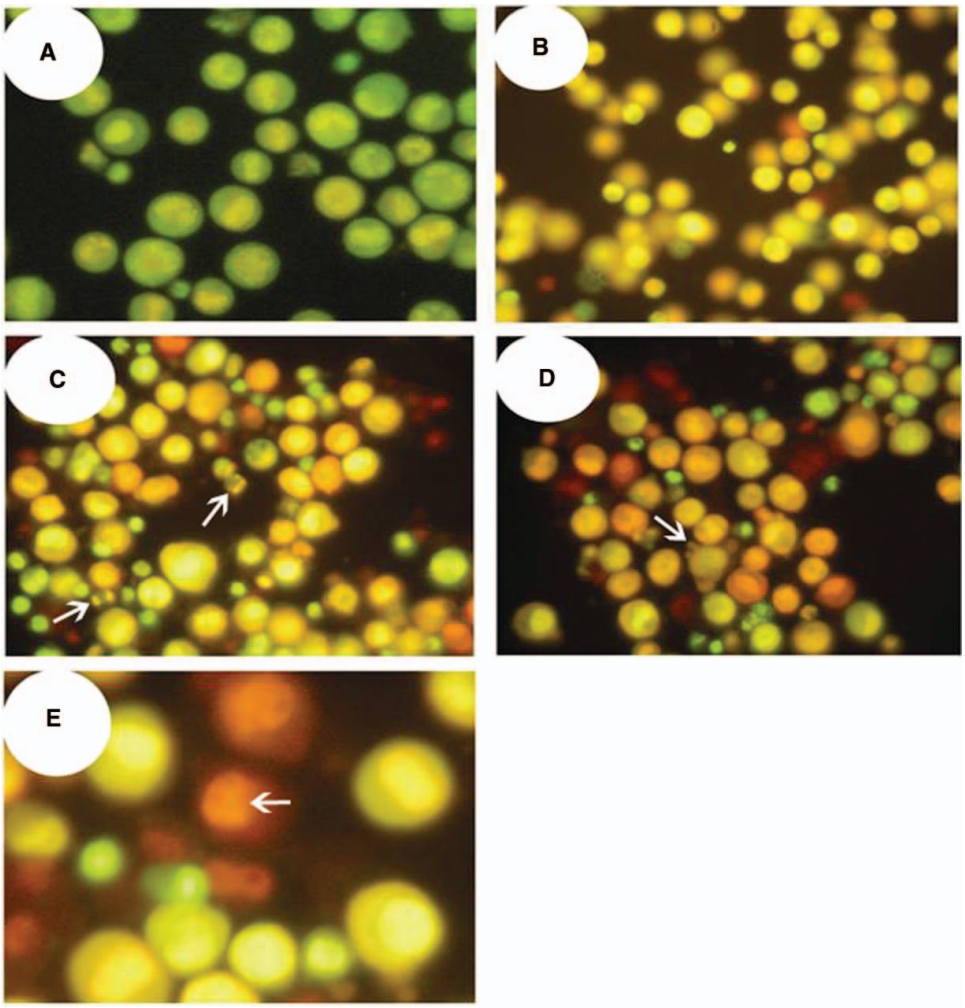

FIGURE 6. DNA laddering assay. L1: marker; L2: DAL-induced tumor cells DNA; L3: tumor cells DNA treated with 600 μg AgNPs; L4: tumor cells treated with 800 μg AgNPs; L5: tumor cells treated with 1000 μg AgNPs; L6: tumor cells treated with aqueous extract of *A. catechu*.

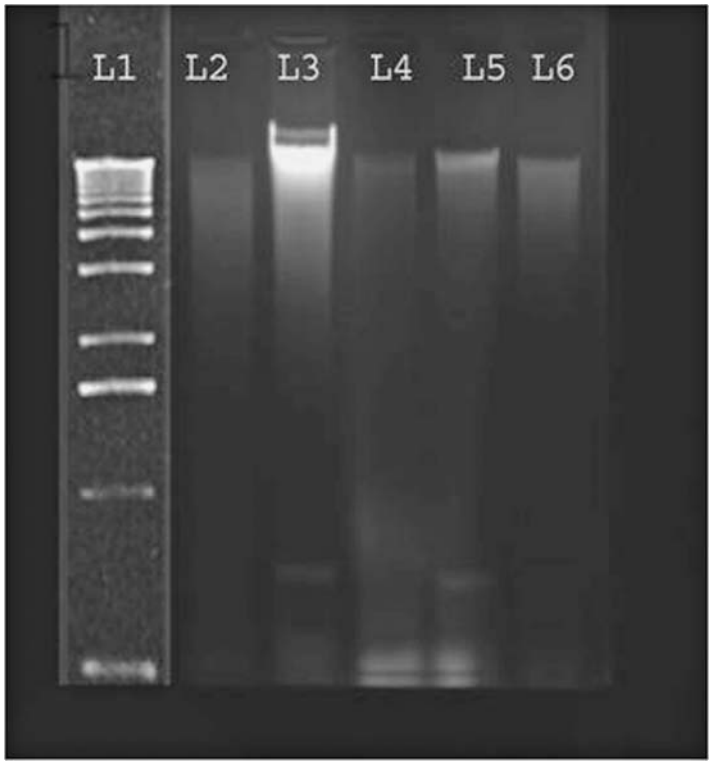

particle size of 85 nm is sufficient to invade tumor cells.[29] Consequently, the particle size of ~85 nm is sufficient to invade the tumor cells.[29] The therapeutic efficacy of biosynthesized AgNPs was significantly different ($p < 0.05$) compared to the aqueous extract–treated group and control group.

Cytotoxicity of Biosynthesized AgNPs

In acridine orange/ethidium bromide (AO/EB) staining, untreated DAL cells exhibited green fluorescence, which reflected their percentage of viability (Figure 5A). A visible nuclear condensation with yellowish orange fluorescence was noticed due to the formation of more apoptotic bodies in the AgNPs-treated DAL cells (Figures 5C, 5D, and 5E) than in the aqueous extract–treated DAL cells (Figure 5B). The formation of blebbing and nuclear condensation was observed in the AgNPs-treated DAL cells exhibiting a reddish orange fluorescence. Our results are in relation to the findings of Yen et al.[31] who predicted that AgNPs are cytotoxic in murine macrophages and fibroblasts.[32] In the present study, AgNPs provoked apoptotic body formation in DAL tumor cells, which is an indispensable indicator of the induction cell death. In addition, DNA fragmentation was observed in AgNPs treated DAL tumor cells in a dose-dependent manner (Figure 6) than the control (lane 2) and aqueous-treated group (lane 6). In the present study, DNA fragments that formed around 100–150 bp revealed that the biosynthesized AgNPs stimulated mitochondrial-mediated apoptosis in DAL cell lines. The previous findings of Yen et al.[31] and Kalishwaralal et al.[33] added sustaining evidence that the formation of a DNA ladder was due to the positive impact of AgNPs.

CONCLUSION

Thus, we concluded that *A. catechu*–derived AgNPs are a novel, cost-effective, potent antitumor agent. The presence of significant polyphenolic content in *A. catechu* was reflected in the efficacy of AgNPs synthesis and its antitumor activity against a DAL mice model. The abundant polyphenolics such as tannins and arecoline (alkaloid) in aqueous extract of *A. catechu* along with the biosynthesized AgNPs confers the synergetic antitumor activity against DAL-induced mice. However, a meticulous study is needed to unravel the molecular mechanism of AgNPs.

EXPERIMENTAL

Materials and Methods

A. catechu Linn. nuts were collected from local surroundings and confirmed by taxonomists. Silver nitrate, acridine orange, ethidium bromide, and agarose were obtained from Sigma (Sigma Aldrich, Bangalore). All other reagents and solvents were analytical grade.

Preparation of Aqueous Extract from A. catechu *Nut*

The nuts were powdered and aqueous solution was prepared by mixing 5 g of nuts with 100 mL of Milli-Q water in a 300 mL Erlenmeyer flask and then boiling the mixture for 10 min. The solutions were filtered and stored at 4°C for one week.

Green Synthesis of AgNPs

Biological synthesis of AgNPs was carried out following Song et al.[19] Typically, 10 mL of aqueous extract was added to 190 mL of 1 mM aqueous silver nitrate solution for the reduction of Ag^+ ions. The effects of temperature on the synthesis rate of the AgNPs were studied by carrying out the reaction at 30–95°C for 10 min. The AgNPs solution thus obtained was purified by repeating the centrifugation thrice at 7000 rpm for 20 min at 4°C followed by redispersion of the pellet in Milli-Q water.

Characterization of AgNPs

UV-visible spectra were recorded as a function of the reaction time on a UV-1650CP spectrophotometer (Shimadzu, Japan) operated at a resolution of 1 nm. The freeze-dried AgNPs' shape and structure were analyzed by SEM (Hitachi Model S3000H). Average particle size of synthesized AgNPs was confirmed by TEM. Briefly, the samples for TEM analysis were prepared by drop-coating AgNPs solutions onto carbon-coated copper TEM grids. The films on the TEM grids were allowed to stand for 2 min, following which the excess solution was removed using blotting paper and the grid was allowed to dry prior to measurement. TEM measurements were performed on a Technai instrument (Technai FE12 Model, Phillips, California) operated at an accelerating voltage at 120 kV. Compositional analysis of the synthesized AgNPs was done by EDX analysis (EDX Thermo Electron Corporation, Massachusetts, USA). The purified AgNPs were examined for the presence of biomolecules using FTIR analysis. The spectrum obtained from the dried sample was recorded on a Spectrum RX 1-One instrument (Perkin-Elmer, USA) in the diffuse reflectance mode at a resolution of 4 cm^{-1} in KBr pellets.

Investigation of Antitumor Activity of Aqueous and Biosynthesized AgNPs

DAL cells were obtained courtesy of Amala Cancer Research Center, Thrissur, Kerala, India. They were maintained by intraperitoneal inoculation of 1×10^6 cells per mouse (Swiss albino male, 30 g body weight) in accordance with the guidelines of animal care of the Institutional Animal Ethical Committee (IAEC), Bharathidasan University, India.

Animal Maintenance

As per standard practice, the mice were quarantined for 15 days before commencement of the experiment. The animals were randomized into four experimental groups excluding normal and control groups ($n = 6$): group 1, normal mice; group 2, tumor-induced mice as control; group 3, tumor-induced mice treated with

A. catechu aqueous extract (2.5 mg/kg BW); group 4, tumor-induced mice treated with AgNPs (600 μg/kg BW); group 5, tumor-induced mice treated with AgNPs (800 μg/kg BW); and group 6, tumor-induced mice treated with AgNPs (1000 μg/kg BW). The antitumor effect of AgNPs and aqueous extract was assessed by observational changes with respect to body weight, tumor volume, and percentage increase in life span. After 10 days of treatment, intraperitoneal ascites fluid was collected from all groups except the normal group and the cells were separated by centrifuging at 3000 rpm for 10 min at 4°C and resuspended in ice-cold phosphate-buffered solution (PBS; pH 7.2) for further studies.

Acridine Orange/Ethidium Bromide (AO/EB) Staining

Tumor cells were collected and washed with PBS and stained by adding 1 mL of AO/EB mix (100 mg/mL AO and 100 mg/mL EB in PBS). After 2 min incubation, cells were washed twice with PBS (5 min each) and visualized under a fluorescence microscope (Olympus 2000, Olympus, Japan) at 400× magnification with an excitation filter 480 nm.

DNA Laddering Assay

A DNA fragmentation assay was performed to analyze the extent of cytotoxicity. Briefly, mice bearing DAL tumor cells were treated with aqueous extract of *A. catechu* and biosynthesized AgNPs for a period of 10 days. The tumor cells were harvested at the end of the experiment and subjected to DNA damage analysis. The isolated cells were washed twice with ice-cold PBS (pH 7.2) and resuspended in Tris-EDTA buffer (20 mM Tris-Hcl at pH 8.0, 20 mM EDTA) containing 0.1% sodium dodecyl sulfate (SDS) and 0.5 mg/mL proteinase K at 50°C for 2 h and then treated with RNase A (0.02 mg/mL) for 30 min at 37°C. DNA was extracted by using phenol/chloroform and precipitated with ethanol further dissolved in distilled water. It was then separated on 1% agarose gel stained with ethidium bromide in which a 100 bp DNA ladder was used as marker (Biotools, Madrid, Spain). The resulting DNA fragmentation was visualized under a UV transilluminator (Medox UV transilluminator [MX 1286-01], India) followed by polarized photography in a gel documentation unit (Model Gs-670, Bio-Rad).

Statistical Analysis

Statistical analysis was done among the experimental groups with control and normal groups using SPSS software version 16 (SPSS Inc., Chicago, Illinois, USA). One-way analysis of variance was performed to express the experimental significance in the present study. Statistical significance was accepted at a level of $p < 0.05$.

REFERENCES

1. Brigger, I.; Dubernet, C.; Couvreur, P. Nanoparticles in cancer therapy and diagnosis. *Adv. Drug Deliv. Rev.* **2002,** *54*, 631–651.

2. Shankar, S. S.; Rai, A.; Ahmad, A.; Sastry, M. Rapid synthesis of Au, Ag, and bimetallic Au core Ag shell nanoparticles using Neem (*Azardica indica*) leaf broth. *J. Colloid Interface Sci*. **2004,** *275*, 496–402.

3. Meenal, K.; Shriwas, A.; Sharmin, K.; Vogel, W.; Urban, J.; Kulkurni, S. K.; Paknikar, K. M. Extracellular synthesis of silver nanoparticles by a silver-tolerant yeast strain MKY3. *J. Nanotechnol*. **2003,** *14*, 95.

4. Klaus, T.; Joergere, R.; Olsson, E.; Granqvist, C. G. Bacteria as workers in the living factory: Metal-accumulating bacteria and their potential for materials science. *Trends Biotechnol*. **2001,** *19*, 15–20.

5. Ahmad, A.; Senapati, S.; Khan, M. I.; Kumar, R.; Sastry, M. Extracellular biosynthesis of monodisperse gold nanoparticles by a novel extremophilic actinomycete, *Thermomonospora* sp. *Langmuir*. **2003,** *19*, 3550–3553.

6. Gardea-Torresdey, L.; Gomez, E.; Peralta-Videa, J. R.; Parsons, J. G.; Troiani, H.; Jose-Yacaman, M.Alfalfa sprouts: A natural source for the synthesis of silver nanoparticles. *Langmuir*. **2003,** *19*, 1357–1361.

7. Gardea-Torresdey, J. L.; Parsons, J. G.; Gomez, E.; Peralta-Videa, J.; Troiani, H. E.; Santiago, P.; Yacaman, M. J. Formation and growth of Au nanoparticles inside alfalfa plants. *Nano Lett*. **2002,** *2*, 397–401.

8. Nazrin Ara, B.; Samiran, M.; Saswati, B.; Rajibul, A. L.; Debabrata, M. Biogenic synthesis of Au and Ag nanoparticles using aqueous extract of black tea extracts. *Colloids and Surfaces B: Biointerfaces*. **2009,** *71*, 113–118.

9. Chandran, S. P.; Chaudhary, M.; Pasricha, R.; Ahmad, A.; Sastry, M. Synthesis of gold nanotriangles and silver nanoparticles using *Aloe vera* plant extract. *Biotechnol. Progr*. **2006,** *22*, 577–583.

10. Shankar, S. S.; Rai, A.; Ahmad, A.; Sastry, M. Controlling the optical properties of lemon grass extract synthesized gold nanotriangles and potential application in infrared-absorbing optical coatings. *Chem. Mater.* **2005,** *17*, 566–572.

11. Shankar, S. S.; Rai, A.; Ahmad, A.; Sastry, M. Rapid synthesis of Au, Ag and bimetallic Au core-Ag shell nanoparticles using neem (*Azadirachta indica*) leaf broth. *J. Colloid Interface Sci.* **2004,** *275*, 496–502.

12. Vilchis-Nestor, A. R.; Sanchez-Mendieta, V.; Camacho-Lopez, M. A.; Gomez-Espinosa, R. M.; Camacho-Lopez, M. A.; Arenas-Alatorre, J. A. Solventless synthesis and optical properties of Au and Ag nanoparticles using *Camellia sinensis* extract. *Mater. Lett*. **2008,** *62*, 3103–3105.

13. Sharan, R. N. Association of *Areca* nut with carcinogenesis a review. *Cancer.* **1996,** *9*, 1.

14. Staples, G. W.; Bevacqua, R. F. *Areca catechu* (betel nut palm). In *Species Profiles for Pacific Island Agroforestry*; Elevitch, C. R., Ed.; Permanent Agriculture Resources: Hôlualoa, Hawaii, 2006; pp. 1–17.

15. Zhang, C. J.; Lv, F. J.; Tai, J. X.; Wang, Z. N.; Fu, Q. Quantitative determination of total phenolics and tannin in areca nut and its products. *Food Dev.* **2008,** *29*, 119–121.

16. Mao, Y.; Park, T. J.; Zhang, F.; Zhou, H.; Wong, S. S. Environmentally friendly methodologies of nanostructure synthesis. *Small.* **2007,** *3*, 1122–1139.

17. Shankar, S. S.; Ahmad, A.; Pasricha, R.; Sastry, M. Bioreduction of chloroaurate ions by geranium leaves and its endophytic fungus yields gold nanoparticles of different shapes. *J. Mater. Chem.* **2003,** *13*, 1822–1826.

18. Sun, Y.; Mayers, B.; Xia, Y. Transformation of silver nanospheres into nanobelts and triangular nanoplates through a thermal process. *Nano Lett.* **2003,** *5*, 675–679.

19. Song, J. Y.; Jang, H. K.; Kim, B. S. Biological synthesis of gold nanoparticles using *Magnolia kobus* and *Diopyros kaki* leaf extracts. *Process Biochem.* **2009,** *44*, 1133–1138.

20. Wiley, B.; Sun, Y.; Mayers, B.; Xia, Y. Shape-controlled synthesis of metal nanostructures: The case of silver. *Chem. Eur. J*. **2005,** *11*, 454–463.

21. Mock, J. J.; Barbic, M.; Smith, D. R.; Schultz, D. A.; Schultz, S. Shape effects in plasmon resonance of individual colloidal silver nanoparticles. *J. Chem. Phys*. **2002,** *116*, 6755–6759.

22. Mukherjee, P.; Ahmad, A.; Mandal, D.; Senapati, S.; Sainkar, S. R.; Khan, M. I.; Ramani, R.; Parischa, R.; Ajaykumar, P. V.; Alam, M.; Sastry, M.; Kumar, R. Bioreduction of $AuCl^{4-}$ ions by the fungus, *Verticillium* sp. and surface trapping of the gold nanoparticles formed. *Angew. Chem. Int. Ed*. **2001,** *40*, 3585–8358.

23. Magudapathy, P.; Gangopadhyay, P.; Panigrahi, B. K.; Nair, K. G. M.; Dhara, S. Electrical transport studies of Ag nanocrystallines embedded in glass matrix. *J. Phys.* **2001,** *299*, 142–146.

24. Song, J. Y.; Kim, B. S. Rapid biological synthesis of silver nanoparticles using plant leaf extract. *Bioproc. Biosystems Eng.* **2009,** *32*, 79–84.

25. Wang, C. K.; Lee, W. H. The separation, characteristics and biological activities of phenolics in areca fruit. *J. Agric. Food Chem.* **1996,** *44*, 2014–2019.

26. Gole, A.; Dash, C.; Ramakrishnan, V.; Sainkar, S. R.; Mandle, A. B.; Rao, M. Pepsin-gold colloid conjugates: Preparation, characterization, and enzymatic. *Langmuir*. **2001,** *17*, 1674–1679.

27. Widowati, S. The use of saponin from *Plumeria acuminatae* Ait as dental pulp tissue devitalization agent (an in vitro study). *TIMNAS FKG UNAIR.* **2005,** *4*, 13–16.

28. Badami, S.; Manohara Reddy, S. A.; Kumar, E. P.; Vijayan, P.; Suresh, B. Antitumor activity of total alkaloid fraction of *Solanum pseudocapsicum* leaves. *Phytother Res*. **2003,** *17*, 1001–1004.

29. EI-Sayed, I. H.; Huang, X.; El-Sayed, M. A. Selective laser photo-thermal therapy of epithelial carcinoma using anti-EGFR antibody conjugated gold nanoparticles. *Cancer Lett*. **2006,** *239*, 129–132.

30. Chanda, N.; Kan, P.; Watkinson, L. D.; Shukla, R.; Zambre, A.; Carmack, T. L.; Engelbrecht, H.; Lever, J. R.; Katti, K.; Fent, G. M.; Casteel, S. W.; Smith, C. J.; Miller, W. H.; Jurisson, S.; Boote, E.; Robertson, J. D.; Cutler, C.; Dobrovolskaia, M.; Kannan, R.; Katti, K. V. Radioactive gold nanoparticles in cancer therapy: Therapeutic efficacy studies GA-^{198}AuNP nanoconstruct in prostate tumor bearing mice. *Nanomedicine.* **2010,** *6*, 201–209.

31. Yen, H. J.; Hsu, S. H.; Tsai, C. L. Cytotoxicity and immunological response of gold and silver nanoparticles of different sizes. *Small.* **2009,** *5*, 1553–1461.

32. Hsin, Y. H.; Chen, C. F.; Haung, S.; Shih, T. S.; Lai, P. S.; Chueh, P. J. The apoptotic effect of nanosilver is mediated by a ROS- and JNK dependent mechanism involving the mitochondrial pathway in NIH3T3 cells. *Toxicol Lett*. **2008,** *179*, 130–139.

33. Kalishwaralal, K.; Banumathi, E.; Ram Kumar Pandian, S.; Deepak, V.; Muniyandi, J.; Eom, S. H.; Gurunathan, S. Silver nanoparticles inhibit VEGF induced cell proliferation and migration in bovine retinal endothelial cells. *Colloids and Surfaces B: Biointerfaces*. **2009,** *73*, 51–57.